Original Article

Acta Radiologica
0(0) 1–10

DOI: 10.1177/0284185116666417
acr.sagepub.com
SAGE

Dynamic contrast-enhanced MRI measurement of renal function in healthy participants

Eli Eikefjord[1,2], Erling Andersen[1,3], Erlend Hodneland[2,4], Erik A Hanson[5], Steven Sourbron[6], Einar Svarstad[2,7], Arvid Lundervold[1,8] and Jarle T Rørvik[1,2]

Abstract

Background: High repeatability, accuracy, and precision for renal function measurements need to be achieved to establish renal dynamic contrast-enhanced magnetic resonance imaging (DCE-MRI) as a clinically useful diagnostic tool.
Purpose: To investigate the repeatability, accuracy, and precision of DCE-MRI measured renal perfusion and glomerular filtration rate (GFR) using iohexol–GFR as the reference method.
Material and Methods: Twenty healthy non-smoking volunteers underwent repeated DCE-MRI and an iohexol–GFR within a period of 10 days. Single-kidney (SK) MRI measurements of perfusion (blood flow, F_b) and filtration (GFR) were derived from parenchymal intensity time curves fitted to a two-compartment filtration model. The repeatability of the SK-MRI measurements was assessed using coefficient of variation (CV). Using iohexol–GFR as reference method, the accuracy of total MR–GFR was determined by mean difference (MD) and precision by limits of agreement (LoA).
Results: SK-F_b (MR1, 345 ± 84; MR2, 371 ± 103 mL/100 mL/min) and SK–GFR (MR1, 52 ± 14; MR2, 54 ± 10 mL/min/1.73 m^2) measurements achieved a repeatability (CV) in the range of 15–22%. With reference to iohexol–GFR, MR–GFR was determined with a low mean difference but high LoA (MR1, MD 1.5 mL/min/1.73 m^2, LoA [−42, 45]; MR2, MD 6.1 mL/min/1.73 m^2, LoA [−26, 38]). Eighty percent and 90% of MR–GFR measurements were determined within ± 30% of the iohexol–GFR for MR1 and MR2, respectively.
Conclusion: Good repeatability of SK-MRI measurements and good agreement between MR–GFR and iohexol–GFR provide a high clinical potential of DCE-MRI for renal function assessment. A moderate precision in MR-derived estimates indicates that the method cannot yet be used in clinical routine.

Keywords
Urinary, MR functional imaging, kidney, adults, imaging sequence, technology assessment

Date received: 2 April 2016; accepted: 3 August 2016

Introduction

Dynamic contrast-enhanced magnetic resonance imaging (DCE-MRI) of the kidneys enables the quantification of renal perfusion and glomerular filtration rate (GFR) in one imaging session (1,2). A number of technical limitations have slowed widespread clinical use of renal DCE-MRI (2–4) and postponed the development and implementation of these quantitative imaging biomarkers (QIB) of renal function. Recently, Sullivan et al. (5) emphasized the need for common standards and terminology in studies on the evaluation

[1]Department of Radiology, Haukeland University Hospital, Bergen, Norway
[2]Department of Clinical Medicine, University of Bergen, Bergen, Norway
[3]Department of Clinical Engineering, Haukeland University Hospital, Bergen, Norway
[4]Christian Michelsen Research (CMR) AS, Bergen, Norway
[5]Department of Mathematics, University of Bergen, Bergen, Norway
[6]Faculty of Medicine and Health, University of Leeds, Leeds, UK
[7]Department of Medicine, Haukeland University Hospital, Bergen, Norway
[8]Department of Biomedicine, University of Bergen, Bergen, Norway

Corresponding author:
Eli Eikefjord, Department of Radiology, Haukeland University Hospital, Bergen, Norway. Jonas Lies vei 65, NO-5021 Bergen, Norway.
Email: eli.eikefjord@hib.no

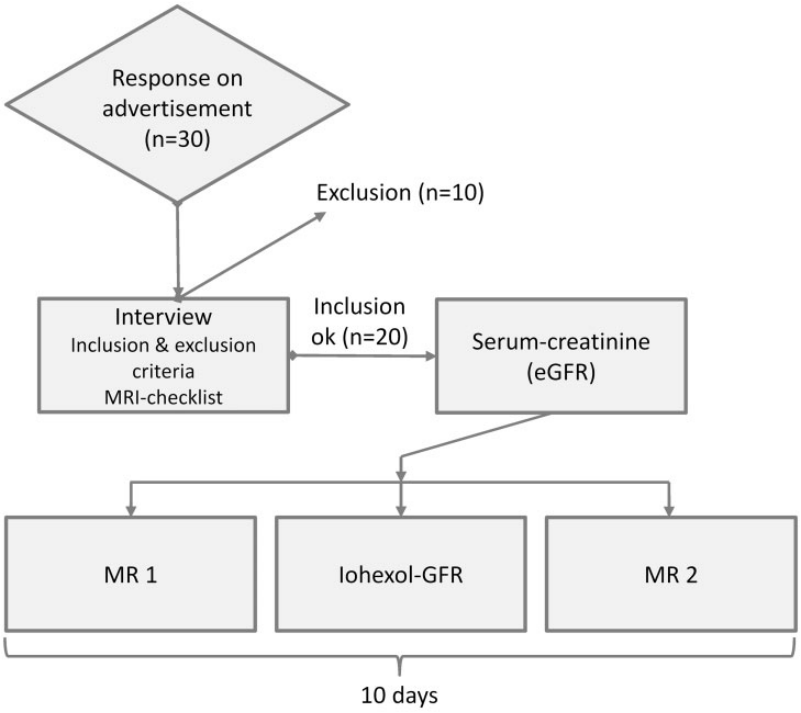

Fig. 1. Enrollment of the participants in the study population.

and comparison of QIB. In this regard, the importance of evaluating technical performance in terms of repeatability and accuracy was emphasized, suggesting an appropriate framework using reference participants, controlled conditions, and reference measurements (5).

For patients, high accuracy for renal DCE-MRI has been reported (2,6–12). For healthy participants, repeatability has been in focus, but accuracy has rarely been studied (13–17). In this work, we simultaneously report repeatability and accuracy for the same healthy participants. In order to validate an MRI-derived GFR biomarker under the criteria of controlled and repeatable conditions, examining healthy participants would be appropriate. Acquiring a GFR reference for healthy participants is achievable using a non-ionizing GFR measurement method. Plasma clearance of ^{51}Cr-EDTA and iohexol are two commonly used GFR measurement methods in Europe (18,19), and they are accepted alternatives to the gold standard method of urinary inulin clearance (20). Iohexol has the advantage of being non-ionizing, stable, cheap, easily available, and non-toxic in the required doses (18).

In our study, repeated DCE-MRI examinations were administered to a sample of healthy volunteers under controlled conditions and using iohexol–GFR as the reference method. Within this framework, we addressed our optimized three-dimensional (3D) DCE-MRI protocol using a repeated breath-hold technique, based on principles described by Lee et al. (21,22). Our aim was to investigate the repeatability of the single-kidney (SK) functional measurements between the two MRI examinations, and to investigate the accuracy and precision of MRI-derived total GFR compared to iohexol–GFR.

Material and Methods

Participants

Twenty healthy non-smoking volunteers were recruited locally and included according to the flow diagram in Fig. 1. The inclusion criteria were normal weight and age under 40 years. Exclusion criteria were a history of renal, hypertensive, or vascular disease, previous moderate or severe allergic reactions to any medication, and the use of any medication. Initially all participants underwent blood tests for Serum-creatinine (SCr). The two DCE-MRI examinations of each individual were undertaken at a fixed interval of 7 days, in accordance with guidelines on the minimum time interval between two gadolinium injections (23). To avoid systematic relations between measurement methods, iohexol–GFR was randomly acquired either prior to MR1, between MR1 and MR2 or after MR2. For practical reasons, the iohexol–GFRs were acquired between 12:00 and 13:00, and both DCE-MRI-examinations between 15:00 and 18:00. Participants were not in a fasting state, but were asked to avoid

alcohol and food with a high protein level, avoid strong physical effort and be normally hydrated for the last 2 days before all examinations, and to have no caffeine on the examination day. Participants were instructed to drink and eat the same type and amount of fluid/food at the same time prior to all examinations to endeavor stable test conditions. The study was approved by our Institutional Review Board, and all participants gave their written informed consent.

Clinical reference serum markers

Iohexol–GFR, which is an established clinical procedure at our Hospital, was used as GFR reference and was performed by injecting 5 mL of iohexol (Omnipaque 300 mg I/mL, GE Healthcare, Oslo, Norway) followed by a venous blood sample after 4 h. The iohexol concentration was analyzed using the single-point method and high-pressure liquid chromatography (HPLC) technique (24). The analytical CV (total over several months) for a similar iohexol–GFR method is reported in the range of 3.3–4.1% (25), assessed by an external quality assurance program (Equalis, Uppsala, Sweden). The patients' erythrocyte volume fraction (EVF) was also measured as part of the iohexol–GFR procedure. The estimated GFR (eGFR) based on enzymatic SCr assays traceable to the isotope dilution mass spectrometry (IDMS) was determined by the Chronic Kidney Disease Epidemiology Collaboration (CKD-EPI Creatinine [2009]) formula (26). The mean interval between SCr and iohexol–GFR was 12 days (standard deviation [SD], 8 days).

MRI

MRI examinations were performed on a 1.5 T scanner (Siemens Magnetom Avanto, Erlangen, Germany) with a gradient strength of 45 mT/m and a slew rate of 200 mT/m/ms, using a standard phased-array coil. Coronal-oblique DCE-MRI data were continuously acquired using a 3D spoiled gradient-recalled (SPGR) pulse-sequence: TE, 0.8 ms; TR, 2.36 ms; flip angle (FA), 20°; parallel imaging factor, 3. Each volume covered the kidneys and the aorta, acquired every 2.3 s for ~6 min with a voxel size of $2.2 \times 2.2 \times 3$ mm^3 and a matrix size of 192×192. A bolus injection of 0.025 mmol/kg of GdDOTA (Guerbet Group, Roissy, France) was administered at 3 mL/s through a 20-G needle placed in an antecubital vein using an automated power injector (Optistar^{LE}, Dublin, Ireland), followed by a 20 mL saline flush. Prior to the injection of gadolinium (Gd), 8 baseline volumes were acquired during an 18-s breath-hold. Seven seconds after the Gd-injection, the participants were instructed to hold the breath for 26 s for motion-free, first pass perfusion. Subsequent instructions for 13-s breath-holds and 26 s of free-breathing were given during the continuous scan for regular motion free intervals throughout filtration phase. Participants received oxygen at a flow of 1 L/min through a nasal cannula to ease breathing.

Image processing and analysis

All DCE-MRI volumes were motion-corrected across time points using a non-parametric automated registration method (27), executed in MATLAB (R2014B). Registered data including all time frames were then analyzed by one operator (4 years of experience of renal DCE analyses) using the software PMI 0.4 (28), written in IDL 6.4. The region of interest (ROI) representing the arterial input function (AIF) was defined semi-automatically on maximum signal-enhancement maps by selecting the 15–20 brightest voxels along the long axis of the aorta, starting just below the orifices of the renal arteries in the mid-coronal slice (Fig. 2). Voxels close to the vessel wall were avoided to minimize potentially partial volume effects.

For each DCE-MRI examination, parenchymal volumes were selected on area under the curve (AUC) maps, excluding extra-renal structures and the renal collecting system.

Assuming a linear relation between signal intensity and the contrast media concentration, contrast media concentration in the aorta $C_A(t)$ and plasma $C_p(t)$ (tissue) was estimated from the signal enhancement $C(t) = S(t) - S_0$, where S_0 is the baseline signal and S(t) is the signal at time t, where S is the mean signal in the parenchymal volume ROI. Such approach has previously been found feasible for the quantification of renal perfusion and filtration measurements using SPGR sequence (6). The concentration-time curves were then fitted to the two-compartment filtration model (2CFM) (29), comprising four independent parameters: plasma volume (V_p), tubular flow (F_t), tubular transit time (T_t), and plasma transit time (T_p), as implemented in PMI (28).

Conversion from plasma (p) to blood (b) was performed in PMI by incorporating the erythrocyte volume fraction (EVF), all parameters presented in units of blood (V_b, T_b). Kidney perfusion, F_b in units of mL/100 mL/min, was derived from the equation $F_b = V_b/T_b$. The glomerular filtration rate, GFR in units of mL/min, was further determined as the product of F_t and the renal parenchymal volume (V_{par}, mL), according to the formula $GFR = F_t\ V_{par}$. For further details on pharmacokinetic model we refer to (29). Total GFR was calculated as the sum of SK–GFR for the left and right kidneys. All GFR measurements were normalized to a body surface area in units of 1.73 m^2 according to the Du Bois

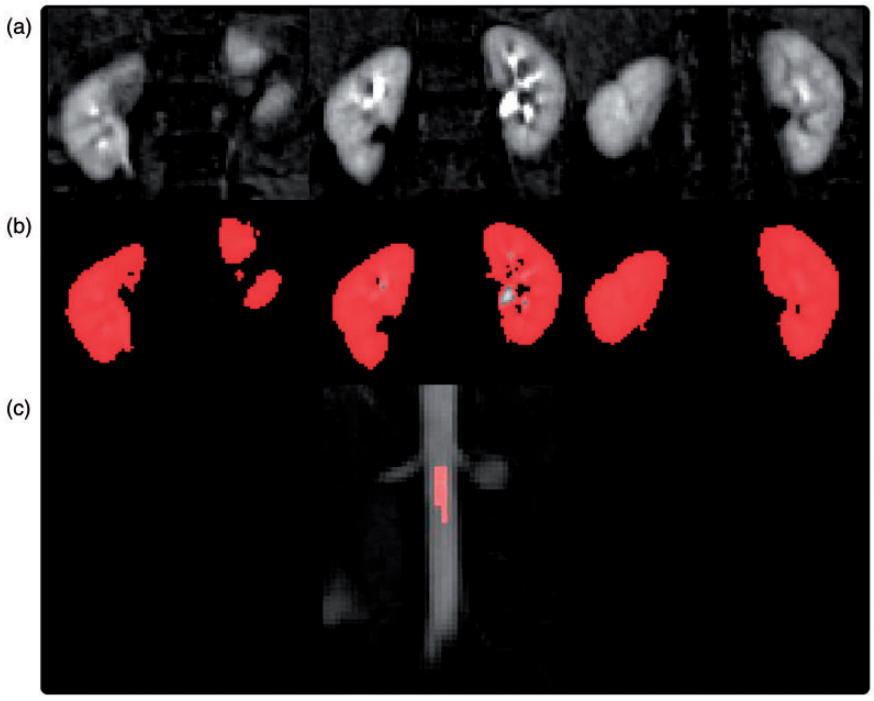

Fig. 2. Method illustration of the area under each pixel curve (AUC) map from three coronal slice positions (a) and corresponding renal parenchymal masks (b). Maximum signal map of the coronal long axis of the aorta is shown in image (c), including localization and size of a typical arterial input mask.

formula: $BSA = 0.007184 \times W^{0}.425 \times H^{0}.725$, where W = weight (kg) and H = height (cm) (30).

Statistical analysis

The repeatability of SK estimates was reported using coefficient of variation (CV), intra-class correlation coefficient (ICC), and Pearson correlation coefficient *r*. CV was calculated as the ratio between the SD of the differences between the measurements from the two imaging sessions and the mean of all the measurements. ICCs was calculated in SPSS using a two-way, random effects ANOVA model measuring the extent of absolute agreement between the test-retest measurements (31).

Accuracy was defined by the two components of uncertainty including both the central tendency (i.e. bias) and data dispersion (i.e. precision). Bias was expressed by the mean difference (MD) and calculated as MR–GFR or eGFR minus iohexol–GFR. Precision was expressed by limits of agreement (LoA), visualized by Bland–Altman plots. Accuracy was also reported as the percentage of eGFR or MR–GFR within ±30% of iohexol–GFR (P30). To ensure consistency with previous validation studies (6–11,13–17), we applied Pearson correlations (*r*) and predictions (regression slope and intercept) of iohexol–GFR from eGFR, and the two DCE-MRI examinations, using a linear regression model.

Statistical significance for all tests was defined at *P* value <0.05. Analyses were performed in Excel 2013 Microsoft, Redmond, WA, USA) using Analyse-it® (Analyse-it Software, Leeds, UK) and SPSS (IBM SPSS 22.0; Armonk, NY, USA).

Results

Clinical characteristics of the study participants are presented in Table 1. Table 2 presents the mean (SD) of the 40 SK measurements derived from MR1 and MR2, including renal blood flow (F_b), tubular flow (F_t), GFR, and renal parenchymal volumes (V_{par}).

The repeatability (CV) of the physiological measurements, F_b, F_t, and GFR, between MR1 and MR2 was in the range of 14.9–21.9%, as presented in Table 2. Correspondingly, ICCs ranged between 0.26 and 0.47 for the measurements, respectively (Table 3). The repeatability of SK volume measurements within participants was 4.4% with an ICC of 0.88.

Fig. 3 visualizes the distribution of individual F_b and SK–GFR measurements at MR1 and MR2. Test–retest Pearson correlations were statistically significant for all measurements except for F_t (Table 3). No systematic differences were observed between the paired measurements, or between the left and right split kidney measurements.

Fig. 4 visualizes the accuracy in terms of agreement between eGFR and iohexol–GFR (Fig. 4a) and between MR–GFR (Fig. 4b, c) and iohexol–GFR. The mean difference between iohexol–GFR and eGFR was 6.8 mL/min/1.73 m^2, whereas mean differences between iohexol–GFR and MR1 and MR1 were 1.5 and 6.1 mL/min/1.73 m^2, respectively. Considerably broader LoA were found in MRI measurements compared to the eGFRs (Table 4). Pearson correlations with iohexol–GFR were comparable for eGFR ($r = 0.56$, $P = 0.011$) and MR1–GFR ($r = 0.57$, $P = 0.010$) and lower for MR2–GFR ($r = 0.29$, $P = 0.229$).

The fraction of GFR measurements quantified by eGFR, MR1, and MR2 that was within P30 of the iohexol–GFR, is presented in Table 4. According to NKF at least 90% of measurements should lie within P30; 100% of the eGFR estimates were found to be within this range, while 80% and 90% of the MR1 and MR2 measurements, respectively, were within this range.

Fig. 5 shows the prediction of iohexol–GFR values from eGFR (Fig. 5a), MR1 and MR2 (Fig. 5b), and Pearson correlations *r*. The fit to the linear model was better for eGFR than both MR1 and MR2. Despite MR1 achieving a slightly better fit than MR2, both imaging sessions were impaired by high unsystematic fluctuations in GFR measurements.

Table 1. Clinical characteristics of study participants.

Variable	Value
Participants (n)	20
Gender (female/male)	16/4
Mean age (years)	25 (20–38)
Height (m)	1.71 ± 0.07
Weight (kg)	66.2 ± 8.7
Body mass index (BMI) (kg/m^2)	22.6 ± 2.1 (18.0–27.0)
Body surface area (BSA) (m^2)	1.77 ± 0.14 (1.5–2.0)
Serum creatinine level (μmoL/L)	70 ± 15 (52–103)
Iohexol–GFR (mL/min/1.73 m^2)	103 ± 10 (87–125)
Estimated GFR (eGFR) (mL/min/1.73 m^2)	110 ± 15 (81–128)
MR1–GFR (mL/min/1.73 m^2)	104 ± 26 (69–154)
MR2–GFR (mL/min/1.73 m^2)	109 ± 16 (84–138)

Parentheses are means and ranges.
Plus-minus values are means ± SD.
GFR, glomerular filtration rate.

Discussion

This study aimed to evaluate repeatability, accuracy, and precision in DCE-MRI derived renal functional measurements. Our results showed that SK perfusion and filtration measurements were repeatable with a CV of 15% and 22%, respectively. With reference to iohexol–GFR, a mean difference of 1.5 and 6.1 mL/min/1.73 m^2 was found in total GFR estimates derived from MR1 and MR2, comparable to findings for eGFR. However, only a moderate precision was found in the MR–GFR measurements expressed by broad limits of agreement compared to iohexol–GFR, indicating unsystematic error sources in our DCE-MRI method.

Day-to-day variations up to 10% can be expected in SCr level associated with factors such as diet and time of day (20,32). The variation in GFR has been found greater in the higher GFR ranges (>90 L/min/1.73 m^2) compared to lower GFR ranges (26).

Our findings of repeatability are in good accordance with previous DCE-MRI studies of healthy volunteers, reporting CVs in perfusion and filtration measurements of 10% and 7% (14), 14% and 18% (13), and 28% (15), respectively. Compared to previous studies using GFR reference to determine accuracy in MR-derived GFR,

Table 2. Mean ± standard deviation (SD) of single-kidney perfusion and filtration measurements derived from MR1 and MR2 in 20 healthy volunteers. The intra-subject repeatability of measurements between MRI examinations is expressed by the coefficient of variation (CV).

	MR1 (mean ± SD)		MR2 (mean ± SD)		CV (%)	
	L	R	L	R	L	R
F_b (mL/100 mL/min)	332 ± 72	358 ± 94	360 ± 90	382 ± 116	21.0	21.9
F_t (mL/100 mL/min)	31 ± 7	35 ± 8	32 ± 5	37 ± 5	18.7	14.9
V_{par} (mL)	161 ± 22	158 ± 19	162 ± 21	162 ± 20	4.2	4.6
SK–GFR (mL/min/1.73 m^2)	49 ± 11	55 ± 16	51 ± 7	58 ± 11	17.5	15.4

F_b, renal blood flow; F_t, tubular flow; L, left kidney; R, right kidney; SK–GFR, single-kidney glomerular filtration rate; V_{par}, renal parenchymal volume.

Table 3. Intra-class correlations (ICC), 95% confidence interval (95% CI), and Pearson correlations (*r*) between the replicated (MR1, MR2) single kidney perfusion and filtration measurements.

	ICC	95% CI	*r*	*P* value
F_b (mL/100 mL/min)	0.34	[0.05, 0.59]	0.36	0.02
F_t (mL/100 mL/min)	0.26	[–0.05, 0.52]	0.26	0.11
V_{par} (mL)	0.88	[0.78, 0.93]	0.88	<0.001
SK–GFR (mL/min/1.73 m^2)	0.47	[0.19, 0.68]	0.51	<0.001

Pearson *r* was considered to be statistically significant at a *P* value of less than 0.05.

F_b, renal blood flow; F_t, tubular flow; SK–GFR, single-kidney glomerular filtration rate; V_{par}, renal parenchymal volume.

our results were in good accordance in terms of the mean difference. Lee et al. (12), Vivier et al. (9), and Lim et al. (6) found mean differences between radioisotope–GFR (^{99}mTc-DTPA) and MR–GFR of −11.9 mL/min, ranging between 4.1 and −7.7 mL/min/1.73 m^2, and of −0.7 mL/min (for SK), respectively. Vivier and colleagues found 95% of the MRI estimates within P30, compared to our results of 80% and 90% for MR1 and MR2, respectively. As regards eGFR, a high P30 (>90%) may be achieved at GFR levels > 90 mL/min/1.73 m^2, in particular using combined equations with cystatin C (33).

Discrepancies were found between our findings and previous studies in terms of strength of associations between MR–GFR estimates and non-MRI reference

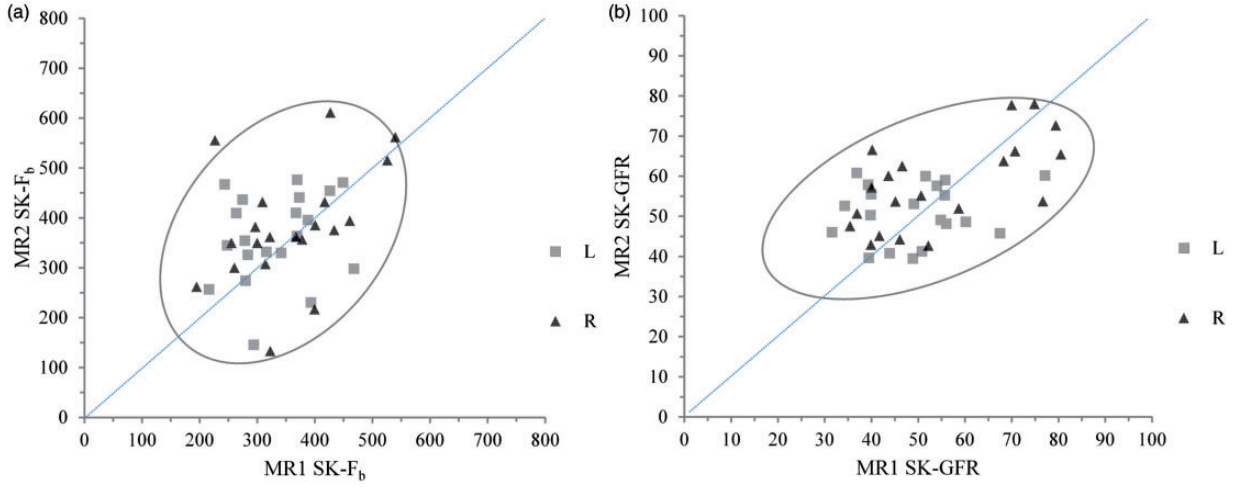

Fig. 3. Correlation plots of the intra-individual perfusion (F_b) and GFR measurements derived from single kidneys at MR1 and MR2. Blood flow, F_b, mL/min/100 mL. Glomerular filtration rate, GFR, mL/min/1.73 m^2. The density ellipses indicate where 95% of the data are expected to lie, whereas a dotted line represents equality. Triangular and square dots represent the right and left kidney, respectively.

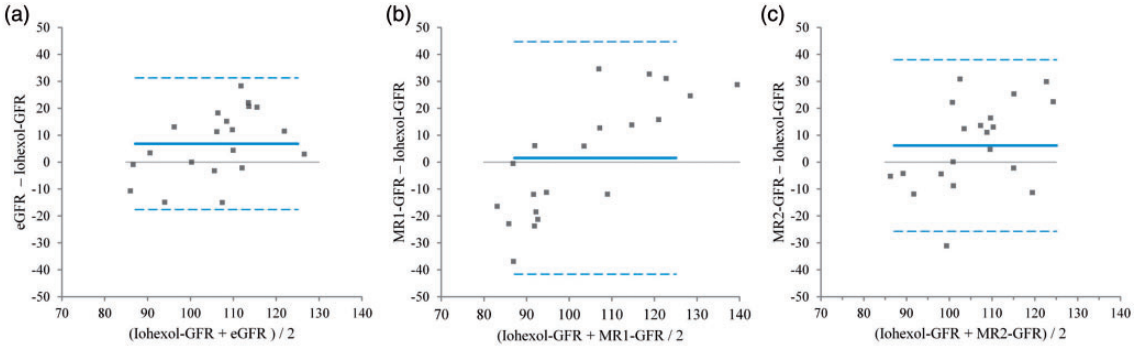

Fig. 4. Bland–Altman plots of the agreement between iohexol–GFR reference values compared to estimated GFR (eGFR) by the CKD-EPI equation (a), MR1 (b) and MR2 (c). All measurements are in mL/min/1.73 m^2. The blue solid line represents the estimated bias (i.e. mean difference, MD), where the zero-bias line is in black. The dashed blue line denotes the mean difference 2SD limits of agreement (LoA).

Table 4. Median difference and percentages of total GFR measurements derived from MR1, MR2, and eGFR that were within plus or minus 30% of iohexol–GFR (P30). Method specific mean differences and limits of agreement are reported with 95% confidence intervals.

	Median difference	P30	Mean difference (bias)	95% CI of mean difference	LoA	95% CI of lower (L) and upper (U) LoA
MR1–GFR	−2.7	80	1.5	−8.6–11.9	−41.6–44.7	L: −59.5–−23.7 U: 26.8–62.6
MR2–GFR	7.9	90	6.1	−1.5–13.8	−25.7–38.0	L: −39.0–12.5 U: 24.8–51.3
eGFR–GFR	7.8	100	6.8	1.0–12.7	−17.6–31.3	L: −27.7–−7.5 U: 21.3–41.4

CI, confidence interval; GFR, glomerular filtration rate, mL/min/1.73 m^2; LoA, limits of agreement.

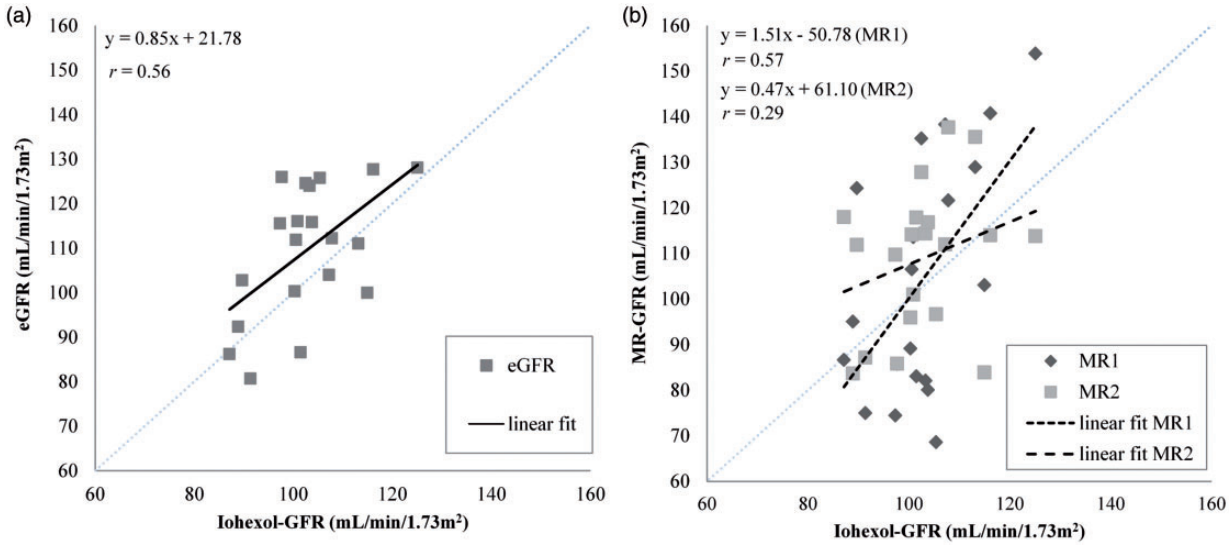

Fig. 5. Relation between SCr based eGFR estimates and iohexol–GFR values (a) and between MR-based GFR estimates and iohexol–GFR values (b). In scatterplots the blue dotted lines indicate equality, and regression lines depicting best linear fit for all data points.

methods. Compared to Lim et al. ($r = 0.91$, slope = 0.96) (6), Buckley et al. ($r = 0.82$, slope = 2.21) (11), Vivier et al. ($c = 0.87$) (9), and Krepkin et al. ($r = 0.87$) (8), our corresponding findings (MR1, $r = 0.57$, slope = 1.51; MR2, $r = 0.29$, slope = 0.47) were substantially weaker. However, our results were consistent with Hackstein et al. (17) examining healthy participants, reporting Pearson $r = 0.36$ between MR–GFR (with similar doses of Gd) and iopromide–GFR. The discrepancy may partly be attributed to the narrow GFR range of the study sample of healthy volunteers.

Several factors may explain the lower absolute agreement (ICC) between the test-retest SK estimates and the lower precision (LoA) between total MR–GFR and iohexol–GFR estimates. The AIF forms the basis for the estimation steps of renal function, and is one factor that has been highlighted for its impact on repeatability and accuracy when high temporal resolution is needed (2,14,34). Measurement errors can originate from sources such as inflow (35) and partial volume effects (3), and mis-registration. Inflow-effects were minimized by using a low flip angle and coronal acquisitions (36), but were still observed in some datasets. This may contribute to a perturbed distribution of the functional estimates. However, other studies are hampered with similar deficiencies, and we have presently no clear explanation of the lower correlations and lower precision found in our study compared to those reported by others.

Retrospective inspection of image data belonging to outliers revealed reconstruction errors (blurring) due to motion in the free-breathing volumes. These effects contributed to fluctuations in the signal-time curves, probably being amplified due to the participants' need to re-oxygenate after breath-holds. Such effects were observed in a few datasets, one case being presented in Fig. 6. Although data were motion corrected in the post-processing phase, breathing effects causing

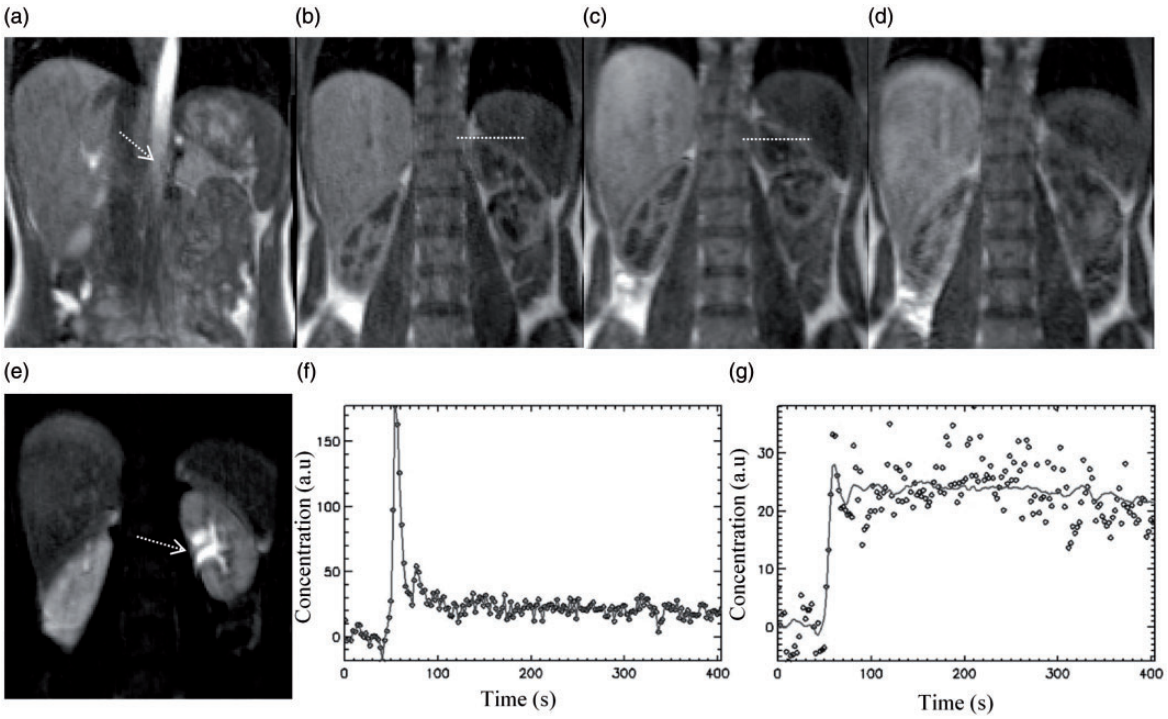

Fig. 6. Presentation of outlier case in terms of deviation in MR–GFR compared to iohexol–GFR (iohexol–GFR: 90 mL/min/1.73 m^2, MR1–GFR: 124 mL/min/1.73 m^2, MR2: 112 mL/min/1.73 m^2) showing: (a) the presence of inflow artifact (arrow) at baseline in nearly the whole length of the aorta; (b, c) alignment artifact between volume frames close in time (~5 s), dotted lines (at same position) indicating difference in kidney positions; (d) mis-positioning of the MRI signal due to reconstruction errors; (e) motion artifacts (arrow) visualized in AUC-map; (f) signal-intensity time curve of the AIF being fairly robustness against motion artifacts; and (g) the kidney signal intensity time curve being prone to highly fluctuating concentrations from baseline throughout the sampling period mainly due to motion effects.

reconstruction errors would likely cause inter-frame mis-registration. As illustrated in Fig. 6, both reconstruction errors and alignment errors are present, leading to erroneous time-curves within the sampling ROIs. Moreover, breathing effects could blur the fine delineation between renal and extra-renal tissue influencing segmentation quality. Although our semi-automatic segmentation procedure required minimal operator involvement and achieved a high ICC (0.88), inclusion and contribution from extrarenal voxels cannot be excluded. Contribution from liver voxels in parenchymal masks has been associated with partial volume effects, significantly influencing function measurements (3). Extensive research efforts have focused on improved motion compensation strategies both in acquisition and post-processing steps in renal DCE-MRI (4,27,37), but no consensus on optimal strategies yet exist.

Our study had several limitations. First, a small study cohort with a homogenous GFR range is presented. A correspondingly increased sensitivity to physiological variation between GFR measurement sessions is expected. Heart rate and blood pressure at the time of MRI examinations could be measured and analyzed in relation to the repeatability of perfusion estimates. Accuracy could probably be increased by performing DCE-MRI measurement and iohexol–GFR measurement at the same day and at the same time of day. Further, a limitation of our study was the assumption of a linear relationship between signal intensity and Gd concentration for the dynamic range of Gd concentrations, although this approach has been previously used in similar studies (6). Compared to our repeated breath-hold technique, a free-breathing protocol would give higher patient compliance when applied to renal disease patients with cardiac or respiratory insuffiency. The moderate precision in our GFR estimates were related to motion effects, emphasizing the importance of developing future robust free-breathing renal DCE-MRI protocols.

In conclusion, our repeated breath-hold DCE-MRI protocol as applied to healthy participants provided single-kidney renal perfusion and GFR measurements with overall good intra-individual repeatability. With reference to iohexol–GFR, MR–GFR achieved low bias, but had only a moderate precision, reflecting high individual variability around values obtained by the reference method. In future studies, using a

framework of repeated DCE-MRI on healthy participants and the use of iohexol–GFR as reference method, may ease validation efforts and facilitate comparisons between studies.

Acknowledgments

The authors would like to thank radiographer Jan Ankar Monssen for valuable discussions and MRI data acquisition, and the renal nurses Liv Unni Kjørvik and Berit Sande at the Renal Outpatient Clinic for organizing and conducting iohexol–GFR measurements. We would also like to acknowledge the MedViz Research Cluster for valuable competence, the Norwegian Research School in Medical Imaging (MedIm) and Bergen University College, Department of Occupational Therapy, Physiotherapy and Radiography, for support.

Declaration of conflicting interests

The authors declared the following potential conflicts of interest with respect to the research, authorship, and/or publication of this article: SOURBRON supervises a PhD student who receives a scholarship jointly funded by Glaxo Smith Kline, Middlesex, UK.

Funding

The authors received the following financial support for the research, authorship, and/or publication of this article: The Regional Health Authority of Western Norway (Helse-Vest) funded this study (grant no. 911713); and the study received grants from the Norwegian Research School in Medical Imaging (MedIm) and from the MedViz Research Cluster.

References

1. Artunc F, Rossi C, Boss A. MRI to assess renal structure and function. Curr Opin Nephrol Hypertens 2011;20: 669–675.
2. Zhang JL, Morrell G, Rusinek H, et al. New magnetic resonance imaging methods in nephrology. Kidney Int 2014;85:768–778.
3. Gutierrez DR, Wells K, Diaz Montesdeoca O, et al. Partial volume effects in dynamic contrast magnetic resonance renal studies. Eur J Radiol 2010;75:221–229.
4. Grenier N, Mendichovszky I, de Senneville BD, et al. Measurement of glomerular filtration rate with magnetic resonance imaging: principles, limitations, and expectations. Semin Nucl Med 2008;38:47–55.
5. Sullivan DC, Obuchowski NA, Kessler LG, et al. Metrology standards for quantitative imaging biomarkers. Radiology 2015;277:813–825.
6. Lim SW, Chrysochou C, Buckley DL, et al. Prediction and assessment of responses to renal artery revascularization with dynamic contrast-enhanced magnetic resonance imaging: a pilot study. Am J Physiol Renal Physiol 2013;305: F672–678.
7. Kang SK, Huang WC, Lee VS, et al. MR renographic measurement of renal function in patients undergoing partial nephrectomy. Am J Roentgenol 2013;200:1204–1209.
8. Krepkin K, Won E, Ramaswamy K, et al. Dynamic contrast-enhanced MR renography for renal function evaluation in ureteropelvic junction obstruction: feasibility study. Am J Roentgenol 2014;202:778–783.
9. Vivier PH, Storey P, Rusinek H, et al. Kidney function: glomerular filtration rate measurement with MR renography in patients with cirrhosis. Radiology 2011;259: 462–470.
10. Yamamoto A, Zhang JL, Rusinek H, et al. Quantitative evaluation of acute renal transplant dysfunction with low-dose three-dimensional MR renography. Radiology 2011;260:781–789.
11. Buckley DL, Shurrab AE, Cheung CM, et al. Measurement of single kidney function using dynamic contrast-enhanced MRI: comparison of two models in human subjects. J Magn Reson Imaging 2006;24: 1117–1123.
12. Lee VS, Rusinek H, Bokacheva L, et al. Renal function measurements from MR renography and a simplified multicompartmental model. Am J Physiol Renal Physiol 2007;292:F1548–1559.
13. Tofts PS, Cutajar M, Mendichovszky IA, et al. Precise measurement of renal filtration and vascular parameters using a two-compartment model for dynamic contrast-enhanced MRI of the kidney gives realistic normal values. Eur Radiol 2012;22:1320–1330.
14. Cutajar M, Mendichovszky IA, Tofts PS, et al. The importance of AIF ROI selection in DCE-MRI renography: reproducibility and variability of renal perfusion and filtration. Eur J Radiol 2010;74:e154–160.
15. Cutajar M, Thomas DL, Hales PW, et al. Comparison of ASL and DCE MRI for the non-invasive measurement of renal blood flow: quantification and reproducibility. Eur Radiol 2014;24:1300–1308.
16. Jorgensen B, Keller AK, Radvanska E, et al. Reproducibility of contrast enhanced magnetic resonance renography in adolescents. J Urol 2006;176:1171–1176.
17. Hackstein N, Kooijman H, Tomaselli S, et al. Glomerular filtration rate measured using the Patlak plot technique and contrast-enhanced dynamic MRI with different amounts of gadolinium-DTPA. J Magn Reson Imaging 2005;22:406–414.
18. Brandstrom E, Grzegorczyk A, Jacobsson L, et al. GFR measurement with iohexol and 51Cr-EDTA. A comparison of the two favoured GFR markers in Europe. Nephrol Dial Transplant 1998;13:1176–1182.
19. Soveri I, Berg UB, Bjork J, et al. Measuring GFR: a systematic review. Am J Kidney Dis 2014;64:411–424.
20. National Kidney Foundation. K/DOQI clinical practice guidelines for chronic kidney disease: evaluation, classification, and stratification. Available at: http://www.ncbi.nlm.nih.gov/pubmed/11904577 (accessed 1 December 2015).
21. Lee VS, Rusinek H, Noz ME, et al. Dynamic three-dimensional MR renography for the measurement of single kidney function: initial experience. Radiology 2003;227:289–294.
22. Bokacheva L, Rusinek H, Zhang JL, et al. Estimates of glomerular filtration rate from MR renography and

tracer kinetic models. J Magn Reson Imaging 2009;29: 371–382.
23. Thomsen HS, Morcos SK, Almen T, et al. Nephrogenic systemic fibrosis and gadolinium-based contrast media: updated ESUR Contrast Medium Safety Committee guidelines. Eur Radiol 2013;23:307–318.
24. Jacobsson L. A method for the calculation of renal clearance based on a single plasma sample. Clin Physiol 1983; 3:297–305.
25. Tøndel CB, Salvador CL, Brackman D, et al. Iohexol plasma clearance in children: validation of multiple formulas and two-point sampling times. Pediatr Nephrol 2016. DOI: 10.1007/s00467-016-3436-z.
26. Levey AS, Stevens LA, Schmid CH, et al. A new equation to estimate glomerular filtration rate. Ann Intern Med 2009;150:604–612.
27. Hodneland E, Lundervold A, Rørvik J, et al. Normalized gradient fields for nonlinear motion correction of DCE-MRI time series. Comput Med Imaging Graph 2014;38: 202–210.
28. Sourbron S, Biffar A, Ingrisch M, et al. PMI: platform for research in medical imaging. Magn Reson Mater Phy 2009;22:539.
29. Sourbron SP, Michaely HJ, Reiser MF, et al. MRI-measurement of perfusion and glomerular filtration in the human kidney with a separable compartment model. Invest Radiol 2008;43:40–48.
30. Verbraecken J, Van de Heyning P, De Backer W, et al. Body surface area in normal-weight, overweight, and obese adults. A comparison study. Metabolism 2006;55: 515–524.
31. Shrout PE, Fleiss JL. Intraclass correlations: uses in assessing rater reliability. Psychol Bull 1979;86:420–428.
32. Bird NJ, Peters C, Michell AR, et al. Reproducibilities and responses to food intake of GFR measured with chromium-51-EDTA and iohexol simultaneously and independently in normal subjects. Nephrol Dial Transplant 2008;23:1902–1909.
33. Bjork J, Grubb A, Larsson A, et al. Accuracy of GFR estimating equations combining standardized cystatin C and creatinine assays: a cross-sectional study in Sweden. Clin Chem Lab Med 2015;53:403–414.
34. Jones RA, Votaw JR, Salman K, et al. Magnetic resonance imaging evaluation of renal structure and function related to disease: technical review of image acquisition, postprocessing, and mathematical modeling steps. J Magn Reson Imaging 2011;33:1270–1283.
35. Zhang JL, Rusinek H, Chandarana H, et al. Functional MRI of the kidneys. J Magn Reson Imaging 2013;37: 282–293.
36. Zeng M, Cheng Y, Zhao B. Measurement of single-kidney glomerular filtration function from magnetic resonance perfusion renography. Eur J Radiol 2015;84: 1419–1423.
37. Zollner FG, Sance R, Rogelj P, et al. Assessment of 3D DCE-MRI of the kidneys using non-rigid image registration and segmentation of voxel time courses. Comput Med Imaging Graph 2009;33:171–181.